Inorg. Chem. **2007**, *46*, 1471–1480

Influence of the Chelate Ligand Structure on the Amide Methanolysis Reactivity of Mononuclear Zinc Complexes

Gajendrasingh K. Ingle,[†] Magdalena M. Makowska-Grzyska,[†] Ewa Szajna-Fuller,[†] Indranil Sen,[†] John C. Price,[†] Atta M. Arif,[‡] and Lisa M. Berreau*[,†]

Department of Chemistry and Biochemistry, Utah State University, Logan, Utah 84322-0300, and Department of Chemistry, University of Utah, Salt Lake City, Utah 84112

Received October 20, 2006

Zinc complexes of three new amide-appended ligands have been prepared and isolated. These complexes, [(dpppa)Zn]$(ClO_4)_2$ (**4**$(ClO_4)_2$; dpppa = *N*-((*N*,*N*-diethylamino)ethyl)-*N*-((6-pivaloylamido-2-pyridyl)methyl)-*N*-((2-pyridyl)methyl)-amine), [(bdppa)Zn]$(ClO_4)_2$ (**6**$(ClO_4)_2$; bdppa = *N*,*N*-bis((*N*,*N*-diethylamino)ethyl)-*N*-((6-pivaloylamido-2-pyridyl)-methyl)amine), and [(epppa)Zn]$(ClO_4)_2$ (**8**$(ClO_4)_2$; epppa = *N*-((2-ethylthio)ethyl)-*N*-((6-pivaloylamido-2-pyridyl)methyl)-*N*-((2-pyridyl)methyl)amine), have been characterized by X-ray crystallography (**4**$(ClO_4)_2$ and **8**$(ClO_4)_2$), ^{1}H and ^{13}C NMR, IR, and elemental analysis. Treatment of **4**$(ClO_4)_2$ or **8**$(ClO_4)_2$ with 1 equiv of $Me_4NOH{\cdot}5H_2O$ in methanol–acetonitrile (5:3) results in amide methanolysis, as determined by the recovery of primary amine-appended forms of the chelate ligand following removal of the zinc ion. These reactions proceed via the initial formation of a deprotonated amide intermediate ([(dpppa$^-$)Zn]ClO_4 (**5**) and [(epppa$^-$)Zn]ClO_4 (**9**)) which in each case has been isolated and characterized (^{1}H and ^{13}C NMR, IR, elemental analysis). Treatment of **6**$(ClO_4)_2$ with $Me_4NOH{\cdot}5H_2O$ in methanol–acetonitrile results in the formation of a deprotonated amide complex, [(bdppa$^-$)Zn]ClO_4 (**7**), which was isolated and characterized. This complex does not undergo amide methanolysis after prolonged heating in a methanol–acetonitrile mixture. Kinetic studies and construction of Eyring plots for the amide methanolysis reactions of **4**$(ClO_4)_2$ and **8**$(ClO_4)_2$ yielded thermodynamic parameters that provide a rationale for the relative rates of the amide methanolysis reactions. Overall, we propose that the mechanistic pathway for these amide methanolysis reactions involves reaction of the deprotonated amide complex with methanol to produce a zinc methoxide species, the reactivity of which depends, at least in part, on the steric hindrance imparted by the supporting chelate ligand. Amide methanolysis involving a zinc complex supported by a N_2S_2 donor chelate ligand (**3**$(ClO_4)_2$) is more complicated, as in addition to the formation of a deprotonated amide intermediate free chelate ligand is present in the reaction mixture.

Introduction

Synthetic zinc complexes of chelate ligands containing the ((6-pivaloylamido-2-pyridyl)methyl)amine component (Figure 1) have been shown to undergo amide methanolysis upon treatment with $Me_4NOH{\cdot}5H_2O$ in methanol-containing solutions.[1−5] Kinetic and mechanistic studies of the amide methanolysis reaction of [(ppbpa)Zn]$(ClO_4)_2$ (**1**$(ClO_4)_2$)[4] in methanol−acetonitrile led to the proposal of a novel reaction

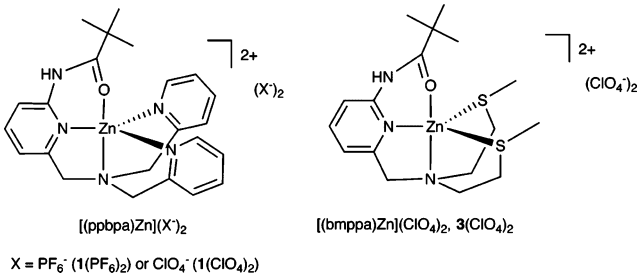

Figure 1. Synthetic zinc complexes containing the ((6-pivaloylamido-2-pyridyl)methyl)amine component for which amide cleavage reactivity has been reported upon treatment of the complex with $Me_4NOH{\cdot}5H_2O$ in methanol-containing solutions.

* To whom correspondence should be addressed. E-mail: berreau@cc.usu.edu. Phone: (435) 797-1625. Fax: (435) 797-3390.
[†] Utah State University.
[‡] University of Utah.

(1) Berreau, L. M.; Makowska-Grzyska, M. M.; Arif, A. M. *Inorg. Chem.* **2000**, *39*, 4390−4391.
(2) Mareque Rivas, J. C.; de Rosales, R. T. M.; Parsons, S. *Dalton Trans.* **2003**, 2156−2163.
(3) Mareque Rivas, J. C.; Salvagni, E.; Prabaharan, R.; de Rosales, R. T. M.; Parsons, S. *Dalton Trans.* **2004**, 172−177.

10.1021/ic062020t CCC: $37.00
Published on Web 01/24/2007

Scheme 1

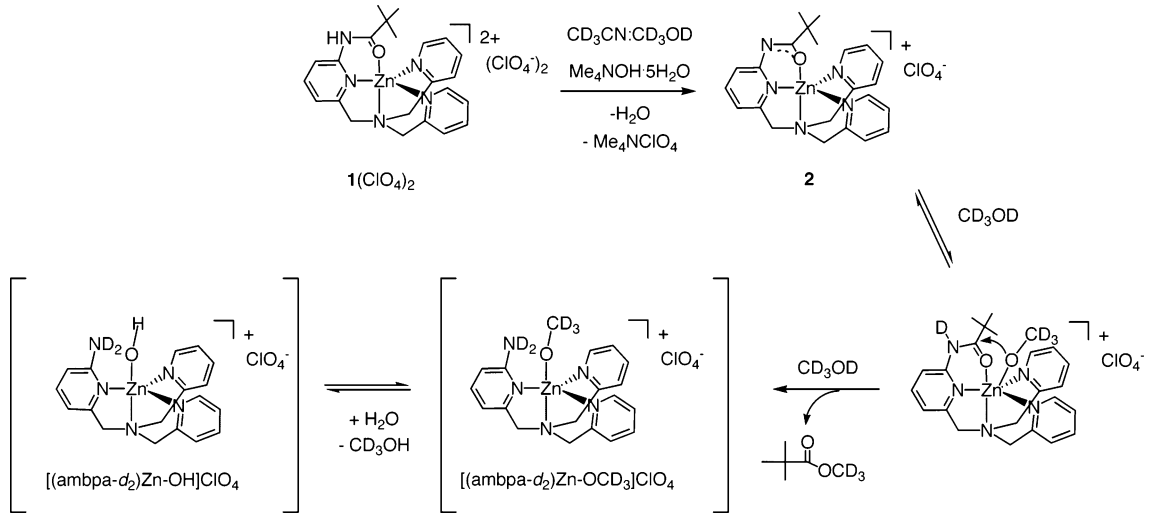

pathway involving a deprotonated amide intermediate, [(ppbpa$^-$)Zn]ClO_4 (**2**; Scheme 1). This intermediate is suggested to undergo reaction with methanol to generate a zinc methoxide species that attacks the amide carbonyl carbon, resulting in the formation of amide methanolysis products.[4] Mareque Rivas and co-workers reported a half-life of 0.41 h for the amide methanolysis reaction of **1**$(ClO_4)_2$ in CD_3OD at 323 K.[3] For the same reaction in CD_3CN-CD_3OD ([CD_3OD] = 15.39 M), a half-life of 0.38 h was determined at 328 K.[4] Preliminary kinetic studies of the amide methanolysis reaction of **3**$(ClO_4)_2$ (Figure 1) in CD_3OD revealed a half-life of 3.95 h.[3] Mareque Rivas and co-workers have argued that the difference in rates of amide methanolysis for these two complexes is the result of differing degrees of amide carbonyl activation by the Zn(II) center.[3]

In the work presented herein, we build on our previously reported kinetic and mechanistic studies of **1**$(ClO_4)_2$[4] and systematically examine how replacement of the unsubstituted pyridyl groups in this complex with various donors affects the amide methanolysis reactivity of mononuclear zinc complexes. The results of this study indicate that increased steric hindrance in the equatorial plane of the zinc cation slows or prevents the amide methanolysis reaction. This is likely due to an influence on the formation and/or reactivity of the zinc methoxide species. Our results also suggest that the slower rate of amide methanolysis for **3**$(ClO_4)_2$ (relative to **1**$(ClO_4)_2$) is due to a side reaction involving the formation of free ligand.

Experimental Section

General and Synthetic Methods. All reagents and solvents were obtained from commercial sources and were used as received unless otherwise noted. The ligand *N*,*N*-bis(2-methylthio)ethyl-*N*-((6-pivaloylamido-2-pyridyl)methyl)amine (bmppa)[6] was prepared as previously described. The ligand precursors 2-(bromomethyl)-6-(pivaloylamido)pyridine[7] and *S*-ethyl-*N*-((2-pyridyl)methyl)aminoethanethiol[8] were prepared according to literature procedures.

Physical Methods. IR spectra were recorded on a Shimadzu FTIR-8400 or a Mattson Polaris FTIR spectrometer as KBr pellets. ^1H and $^{13}C\{^1H\}$ NMR spectra for compound characterization were recorded at 20(1) °C on a JEOL GSX-270, JEOL ECX-300, or Bruker ARX400 spectrometer. Chemical shifts (ppm) are referenced to the residual solvent peak(s) in C*H*D_2CN (^1H, 1.94 (quintet); $^{13}C\{^1H\}$, 1.39 (heptet) ppm). Kinetic studies were performed by ^1H NMR on a JEOL GSX-270 or JEOL ECX-300 NMR spectrometer having a thermally regulated probe. A temperature calibration curve was recorded for the temperature ranges of 297−358 K (JEOL GSX-270) and 295−353 K (JEOL ECX-300) using ethylene glycol. Further details of the ^1H NMR kinetic studies are available in the Supporting Information. Fast atom bombardment (FAB) mass spectra were obtained at the University of California, Riverside, using a VG ZAB2SE high-resolution mass spectrometer in a matrix of *m*-nitrobenzyl alcohol (MNBA). Elemental analyses were performed by Atlantic Microlabs of Norcross, GA.

Caution: *Perchlorate salts of metal complexes with organic ligands are potentially explosive. Only small amounts of material should be prepared, and these should be handled with great care.*[9]

***N*-((*N*,*N*-Diethylamino)ethyl)-*N*-((2-pyridyl)methyl)amine.** This compound has been previously reported, albeit a detailed synthetic procedure was not provided.[10] To an ethanol (100 mL) solution of *N*,*N*-diethylethylenediamine (5.7 g, 4.9×10^{-2} mol) was added 2-pyridylcarboxaldehyde (5.3 g, 4.9×10^{-2} mol). The resulting solution was heated under a nitrogen atmosphere at 40(1) °C for 1 h. The reaction mixture was then cooled to ambient temperature, and $NaBH_4$ (2.2 g, 5.9×10^{-2} mol) was added. The solution was then stirred for ∼12 h at ambient temperature. The pH was adjusted to ∼2 using first 1 M HCl followed by a few drops of concentrated hydrochloric acid. The ethanol was removed under reduced pressure. Addition of 1 M NaOH (100 mL) to the remaining brown aqueous solution, followed by extraction with Et_2O (3 × ∼100 mL), drying

(4) Szajna, E.; Makowska-Grzyska, M. M.; Wasden, C. C.; Arif, A. M.; Berreau, L. M. *Inorg. Chem.* **2005**, *44*, 7595−7605.
(5) The acronym used for the ppbpa ligand in refs 2 and 3 is bppapa.
(6) Berreau, L. M.; Allred, R. A.; Makowska-Grzyska, M. M.; Arif, A. M. *Chem. Commun*. **2000**, 1423−1424.
(7) Berreau, L. M.; Mahapatra, S.; Halfen, J. A.; Young, V. G., Jr.; Tolman, W. B. *Inorg. Chem.* **1996**, *35*, 6339−6342.
(8) Funahashi, Y.; Kato, C.; Yamauchi, O. *Bull. Chem. Soc. Jpn.* **1999**, *72*, 415−424.
(9) Wolsey, W. C. *J. Chem. Educ.* **1973**, *50*, A335−A337.
(10) Sarkar, S.; Mondal, A.; Ribas, J.; Drew, M. G. B.; Pramanik, K.; Rajak, K. K. *Inorg. Chim. Acta* **2005**, *358*, 641−649.
(11) Wilkins, R. G. *Kinetics and Mechanism of Reactions of Transition Metal Complexes*, 2nd ed.; VCH Publishers: New York, 1991.

of the organic extracts over Na_2SO_4, and removal of the solvent under reduced pressure, yielded a dark brown oil. The product was purified by Kugelrohr distillation at 105−110 °C at 3 mmHg, which yielded a yellow oil (2.9 g, 29%): ^{1}H NMR (CD_3CN, 270 MHz) δ 8.48 (d, J = 4.6 Hz, 1H), 7.79−7.64 (m, 1H), 7.34 (d, J = 7.9 Hz, 1H), 7.22−7.15 (m, 1H), 3.82 (s, 2H), 2.65−2.40 (m, 8H), 0.97 (t, J = 7.2 Hz, 6H); ^{13}C{^{1}H} NMR (CD_3CN, 100 MHz) δ 161.9, 150.1, 137.4, 122.9, 122.8, 56.0, 53.8, 48.0, 47.9, 12.5 (10 signals expected and observed); FTIR (neat, cm^{-1}) ∼3305 (br, ν_{N-H}); LREI-MS (NH_3) m/z (relative intensity) 208 ([M + H]$^+$, 100).

***N*-((*N*,*N*-Diethylamino)ethyl)-*N*-((6-pivaloylamido-2-pyridyl)methyl)-*N*-((2-pyridyl)methyl)amine (dpppa).** To a round-bottom flask containing *N*-((*N*,*N*-diethylamino)ethyl)-*N*-((2-pyridyl)methyl)-amine (0.87 g, 4.2 × 10^{-3} mol) were added 2-(bromomethyl)-6-(pivaloylamido)pyridine (1.14 g, 4.2 × 10^{-3} mol), sodium carbonate (1.1 g, 1.0 × 10^{-2} mol), and tetrabutylammonium bromide (∼5 mg). Acetonitrile (50 mL) was added to the flask, and the solution was heated at reflux for 20 h, at which point the reaction mixture was brown in color. The solution was then cooled to room temperature, and 1 M NaOH (50 mL) was added. This solution was extracted with CH_2Cl_2 (3 × ∼60 mL), the combined organic fractions were dried over Na_2SO_4, and the solvent was removed in vacuo. The remaining dark brown oil was purified by column chromatography on silica gel (230−400 mesh, methanol, $R_f \approx 0.3$ (long trailing band)) to yield a dark yellow thick oil (0.87 g, 52%): ^{1}H NMR (CD_3CN, 400 MHz) δ 8.50−8.45 (m, 1H), 8.12 (br, 1H, NH), 7.97 (d, J = 8.3 Hz, 1H), 7.72−7.67 (m, 2H), 7.56 (d, J = 7.9 Hz, 1H), 7.29 (d, J = 7.5 Hz, 1H), 7.20−7.15 (m, 1H), 3.81 (s, 2H), 3.72 (2H), 2.60−2.55 (m, 4H), 2.40 (q, J = 7.1 Hz, 4H), 1.27 (s, 9H), 0.91 (t, J = 7.1, 6H); ^{13}C{^{1}H} NMR (CD_3CN, 100 MHz) δ 177.9, 161.2, 159.9, 152.2, 149.8, 139.5, 137.3, 123.8, 122.9, 119.5, 112.5, 61.7, 61.3, 53.3, 52.1, 48.2, 40.4, 27.6, 12.5 (19 signals expected and observed); FTIR (neat, cm^{-1}) 1689 ($\nu_{C=O}$); LRFAB-MS (NBA) m/z (relative intensity) 398 ([M + H]$^+$, 100).

***N*,*N*-Bis((*N*,*N*-diethylamino)ethyl)-*N*-((6-pivaloylamido-2-pyridyl)methyl)amine (bdppa).** To a 250 mL round-bottom flask were added 2-(bromomethyl)-6-(pivaloylamido)pyridine (3.43 g, 12.6 mmol), *N*,*N*,*N*′,*N*′-tetraethyldiethylenetriamine (2.72 g, 12.6 mmol), Na_2CO_3 (4.60 g), and tetrabutylammonium bromide (∼5 mg). To this mixture of solids was added CH_3CN (100 mL). The solution was heated at reflux under a nitrogen atmosphere for 20 h. At this point, the solution was cooled to ambient temperature, and ∼12 mL of 1 M NaOH was added. The entire mixture was extracted with CH_2Cl_2 (3 × 100 mL). The combined organic fractions were dried over Na_2SO_4, filtered, and brought to dryness by rotary evaporation. The resulting dark brown oil was purified by column chromatography on silica gel (230−400 mesh, methanol, $R_f \approx 0.2$) to yield a yellow-brown solid (3.36 g, 65%): ^{1}H NMR (CD_3CN, 400 MHz) δ 8.15 (br s, 1H, N*H*), 7.97 (d, J = 8.2 Hz, 1H), 7.67 (t, J = 7.9 Hz, 1H), 7.22 (d, J = 7.5 Hz, 1H), 3.66 (s, 2H), 2.58−2.49 (m, 8H), 2.45 (q, J = 7.1 Hz, 8H), 1.26 (s, 9H), 0.94 (t, J = 7.1 Hz, 12H); ^{13}C{^{1}H} NMR (CD_3CN, 100 MHz) δ 177.9, 160.4, 152.1, 139.4, 119.6, 112.5, 61.8, 53.8, 52.2, 47.9, 40.5, 27.7, 12.5 (13 signals expected and observed); FTIR (neat, cm^{-1}) 1691 ($\nu_{C=O}$); LRFAB-MS (CH_3OH−NBA−NaCl) m/z (relative intensity) 428 ([M + Na]$^+$, 100), 406 ([M + H]$^+$, 25).

***N*-((2-Ethylthio)ethyl)-*N*-((6-pivaloylamido-2-pyridyl)methyl)-*N*-((2-pyridyl)methyl)amine (epppa).** To a round-bottom flask containing *S*-ethyl-*N*-((2-pyridyl)methyl)aminoethanethiol (1.25 g, 6.38 mmol) were added 2-(bromomethyl)-6-(pivaloylamido)pyridine (1.75 g, 6.46 mmol), sodium carbonate (1.39 g, 13.1 mmol), and tetrabutylammonium bromide (∼5 mg). Acetonitrile (100 mL) was added to the flask, and the solution was heated at reflux for 12 h. Purification by column chromatography on silica gel (230−400 mesh, ethyl acetate, $R_f \approx 0.8$) yielded a pale yellow solid (1.63 g, 66%): ^{1}H NMR (CD_3CN, 270 MHz) δ 8.45 (d, J = 4.9 Hz, 1H), 8.15 (br, 1H), 7.98 (d, J = 7.9 Hz, 1H), 7.74−7.62 (m, 2H), 7.56 (d, J = 7.9 Hz, 1H) 7.29 (d, J = 7.6 Hz, 1H), 7.22−7.12 (m, 1H), 3.80 (s, 2H), 3.70 (s, 2H), 2.78−2.60 (m, 4H), 2.41 (quartet, J = 7.2 Hz, 2H), 1.26 (s, 9H), 1.13 (t, J = 7.2 Hz, 3H); ^{13}C{^{1}H} NMR (CD_3CN, 67.9 MHz) δ 178.9, 161.7, 160.4, 153.1, 150.8, 140.5, 138.3, 124.9, 124.0, 120.5, 113.6, 61.9, 61.6, 55.8, 41.4, 30.6, 28.6, 27.4, 16.3 (19 signals expected and observed); FTIR (neat, cm^{-1}) 1688 ($\nu_{C=O}$); LRFAB-MS (CH_3OH−NBA) m/z (relative intensity) 387 ([M + H]$^+$, 100). Anal. Calcd for $C_{21}H_{30}N_4OS$: C, 65.25; H, 7.83; N, 14.50. Found: C, 65.12; H, 7.90; N, 14.19.

[(dpppa)Zn](ClO$_4$)$_2$ (4(ClO$_4$)$_2$). To a solution of $Zn(ClO_4)_2 \cdot 6H_2O$ (0.094 g, 0.25 mmol) in methanol (∼5 mL) was added a methanol solution (∼5 mL) of dpppa (0.10 g, 0.25 mmol). The resulting clear, colorless mixture was stirred at ambient temperature for ∼60 min. Following addition of excess Et_2O (∼80 mL), a white powder was deposited. Recrystallization of this white powder by diethyl ether diffusion into a CH_3CN solution yielded colorless needles and plates (yield 72%). Crystals suitable for single-crystal X-ray diffraction analysis were obtained by recrystallization of the isolated material from CH_3CN−CH_3OH−Et_2O: ^{1}H NMR (CD_3CN, 400 MHz) δ 9.51 (br, 1H), 8.56−8.52 (m, 1H), 8.20−8.10 (m, 2H), 7.72−7.64 (m, 1 H), 7.60 (d, J = 7.9 Hz, 1H), 7.53 (d, J = 8.2 Hz, 1H), 7.44 (d, J = 7.6 Hz, 1H), 4.55 (d, J = 17 Hz, 1H), 4.36 (s, 2H), 4.14 (d, J = 17 Hz, 1H), 3.40−2.70 (m, 8H), 1.48 (s, 9H), 1.26 (t, J = 7.2 Hz, 3H), 1.01 (t, J = 7.2 Hz, 3H); ^{13}C{^{1}H} NMR (CD_3CN, 100 MHz) δ 187.0, 156.6, 154.8, 152.5, 148.7, 144.8, 143.2, 126.8, 126.1, 122.7, 117.6, 59.5, 57.5, 52.6, 52.3, 49.1, 48.5, 42.6, 27.3, 11.5, 8.2 (21 signals expected and observed); FTIR (KBr, cm^{-1}) 3325 (br, ν_{N-H}), 1652, 1623, 1095 (ν_{ClO_4}), 623 (ν_{ClO_4}); LRFAB-MS (CH_3CN−NBA) m/z (relative intensity) 560 ([M − ClO$_4$]$^+$, 10). Anal. Calcd for $C_{23}H_{35}N_5O_9Cl_2Zn$: C, 41.87; H, 5.35; N, 10.62. Found: C, 41.86; H, 5.32; N, 10.48.

[(bdppa)Zn](ClO$_4$)$_2$ (6(ClO$_4$)$_2$). This compound was prepared in a manner identical to that of **4**(ClO$_4$)$_2$. Recrystallization of the crude white powder via diethyl diffusion into an ^{i}PrOH−CH_3CN (1:2) solution yielded a white polycrystalline material (yield 84%): ^{1}H NMR (CD_3CN, 400 MHz) δ 9.49 (br s, 1H, N*H*), 8.17 (t, J = 8.0 Hz, 1H), 7.54 (d, J = 8.2 Hz, 1H), 7.44 (d, J = 7.7 Hz, 1H), 4.26 (s, 2H), 3.30−2.80 (m, 14H), 2.55−2.35 (br, 2H), 1.41 (s, 9H), 1.36−1.15 (br m, 6H), 1.11−0.80 (br m, 6H); ^{13}C{^{1}H} NMR (CD_3CN, 400 MHz) δ 186.2, 155.5, 152.0, 144.9, 122.9, 117.8, 58.7, 52.6, 52.0, 48.9, 47.1, 42.4, 27.2, 10.7, 7.3 (15 resonances expected and observed); FTIR (KBr, cm^{-1}) 3369 (br, ν_{N-H}), 1634, 1623, 1532, 1089 (ν_{ClO_4}), 623 (ν_{ClO_4}); LRFAB-MS (CH_3OH−NBA) m/z (relative intensity) 468 ([M − H]$^+$, 100). Anal. Calcd for $C_{23}H_{43}N_5O_9Cl_2Zn$: C, 41.37; H, 6.50; N, 10.49. Found: C, 41.13; H, 6.46; N, 10.50.

[(epppa)Zn](ClO$_4$)$_2$ (8(ClO$_4$)$_2$). This compound was prepared in a manner identical to that of **4**(ClO$_4$)$_2$. Recrystallization of the crude white powder by diethyl ether diffusion into an ^{i}PrOH−CH_3-OH (1:1) solution yielded colorless prisms (yield 97%): ^{1}H NMR (CD_3CN, 400 MHz) δ 9.51 (br, 1H, N*H*), 8.56 (d, J = 5.4 Hz, 1H), 8.18−8.10 (m, 2H), 7.70 (t, J = 8.6 Hz, 1H), 7.65 (d, J = 8.3 Hz, 1H), 7.54 (d, J = 8.3 Hz, 1H), 7.36 (d, J = 8.3 Hz, 1H), 4.46 (d, J = 16. 8 Hz, 1H), 4.36 (d, J = 16.8 Hz, 1H), 4.26 (d, J = 16.8 Hz, 1H), 4.22 (d, J = 16.8 Hz, 1H), 3.35−3.18 (m, 1H), 3.10−2.87 (m, 3H), 2.48 (quartet, J = 7.3 Hz, 2H), 1.49 (s, 9H), 1.27 (t, J = 7.3 Hz, 3H); ^{13}C{^{1}H} NMR (CD_3CN, 100 MHz) δ 186.7, 155.7, 153.8, 152.4, 148.8, 144.8, 143.2, 126.8, 126.3, 122.5, 117.4,

59.0, 57.8, 52.6, 42.6, 30.8, 27.3, 26.9, 13.7 (19 resonances expected and observed); FTIR (KBr, cm^{-1}) 3331 (br, ν_{N-H}), 1646, 1624, 1612, 1573, 1530, 1097 (ν_{ClO_4}), 623 (ν_{ClO_4}); LRFAB-MS (CH_3OH−NBA) *m*/*z* (relative intensity) 449 ($[M - H]^+$, 100). Anal. Calcd for $C_{21}H_{30}N_4O_9SCl_2Zn$: C, 38.89; H, 4.67; N, 8.64. Found: C, 38.70; H, 4.65; N, 8.58.

[(dpppa)Zn](OTf)$_2$ (4(OTf)$_2$), [(bdppa)Zn](OTf)$_2$ (6(OTf)$_2$), and [(epppa)Zn](OTf)$_2$ (8(OTf)$_2$). All of these compounds have been prepared and purified in a manner identical to that of **1**$(OTf)_2$.[4] Spectroscopic data for these triflate analogues is available in the Supporting Information.

[(dpppa$^-$)Zn]ClO$_4$ (5). To a solution of **4**$(ClO_4)_2$ (0.043 g, 0.065 mmol) in methanol (∼3 mL) was added $Me_4NOH·5H_2O$ (0.012 g, 0.066 mmol) dissolved in methanol (∼5 mL) and acetonitrile (∼2 mL). The resulting mixture was stirred for ∼2−3 min at room temperature. The solvent was then removed under reduced pressure. The remaining solid was redissolved in CH_2Cl_2, the solution was filtered, and the filtrate was brought to dryness under reduced pressure. The solid was again redissolved in CH_2Cl_2 (∼2 mL) and precipitated by the addition of excess diethyl ether (∼10 mL). Drying of the precipitate under vacuum yielded a white solid (yield 64%): ^{1}H NMR (CD_3CN, 400 MHz) δ 8.63 (d, J = 5.2 Hz, 1H), 8.08 (dt, J_1 = 8.0 Hz, J_2 = 1.6 Hz, 1H), 7.71 (t, J = 8.0 Hz, 1H), 7.65−7.60 (m, 1H), 7.53 (d, J = 7.9 Hz, 1H), 6.88 (d, J = 7.8 Hz, 1H), 6.86 (d, J = 8.5 Hz, 1H), 4.36 (d, J = 17 Hz, 1H), 4.15 (d, J = 17 Hz, 1H), 4.05 (d, J = 17 Hz, 1H), 4.04 (d, J = 17 Hz, 1H), 3.10−2.90 (m, 2H), 2.75−2.59 (m, 6H), 1.30 (s, 9H), 1.10 (t, J = 7.2 Hz, 6H) (a ^{1}H−^{1}H COSY spectrum of **5** indicated that the methylene protons of the diethylamine donor appendage are located in the signal at 2.75−2.59 ppm); ^{13}C{^{1}H} NMR (CD_3CN, 100 MHz) δ 185.2, 163.4, 157.0, 152.0, 148.7, 142.5, 142.1, 126.4, 125.7, 123.6, 116.4, 59.0, 57.8, 51.8, 48.9, 41.9, 29.3, 10.0 (HMQC studies indicate that the N*C*H$_2$*C*H$_3$ carbons are overlapped in signals at 48.9 and 10.0 ppm, respectively, in the ^{13}C{^{1}H} spectrum; these studies also indicate that the methylene linker carbons of the *N*,*N*-(diethylamino)ethyl appendage overlap in a signal at 51.8 ppm in the ^{13}C{^{1}H} spectrum); FTIR (KBr, cm^{-1}) 1609, 1567, 1492, 1451, 1095 (ν_{ClO_4}), 623 (ν_{ClO_4}). Anal. Calcd for $C_{23}H_{34}N_5O_5ClZn$: C, 49.36; H, 6.13; N, 12.52. Found: C, 49.91; H, 6.36; N, 12.06. Trace Et_2O (∼0.25 equiv) was present in the elemental analysis sample as indicated by ^{1}H NMR. Inclusion of this solvent in the calculated values produces a more satisfactory fit to the experimentally determined analytical data. Anal. Calcd for $C_{21}H_{29}N_4O_5SClZn·0.25Et_2O$: C, 49.86; H, 6.37; N, 12.12. Found: C, 49.91; H, 6.36; N, 12.06.

[(bdppa$^-$)Zn]ClO$_4$ (7). To bdppa (0.061 g, 0.15 mmol) dissolved in methanol−acetonitrile (3:2, 10 mL) was added $Zn(ClO_4)_2·6H_2O$ (0.055 g, 0.15 mmol) dissolved in methanol (∼3 mL). The resulting mixture was stirred for 15 min at room temperature. This solution was then added to solid $Me_4NOH·6H_2O$ (0.027 g, 0.15 mmol), and the resulting mixture was stirred for 2 h. The solvent was removed under vacuum. The remaining solid was dissolved in CH_2Cl_2, and the solution was filtered through a Celite/glass wool plug. The filtrate was brought to dryness under vacuum. The remaining solid was washed with diethyl ether and then dried under vacuum (yield 49%): ^{1}H NMR (CD_3CN, 300 MHz) δ 7.74 (t, J = 7.8 Hz, 1H), 6.87 (d, J = 7.8 Hz, 2H), 3.97 (s, 2H), 3.11−2.60 (br m, 14 H), 2.50−2.32 (br, 2H), 1.25 (t, J = 7.0 Hz, 6H), 1.21 (s, 9H), 0.86 (t, J = 7.0 Hz, 6H); ^{13}C{^{1}H} NMR (CD_3CN, 100 MHz) δ 184.4, 152.5, 142.3, 123.1, 116.5, 58.5, 52.1, 51.5, 48.8, 46.9, 41.6, 29.0, 10.0, 8.0 (15 signals expected, 14 observed; two overlapping aromatic resonances at 142.3 ppm); FTIR (KBr, cm^{-1}) 1604, 1566, 1494, 1443, 1104, 1081, 623 (ν_{ClO_4}). Anal. Calcd for $C_{23}H_{42}N_5O_5ClZn$: C, 48.66; H, 7.46; N, 12.34. Found: C, 48.46; H, 7.45; N, 12.27.

[(epppa$^-$)Zn]ClO$_4$ (9). This compound was prepared and isolated in a manner identical to that of **5** (starting from **8**$(ClO_4)_2$) except the reaction was performed in acetonitrile (yield 81%): ^{1}H NMR (CD_3CN, 300 MHz) δ 8.61 (m, 1H), 8.09 (t, J = 7.6 Hz, 1H), 7.76 (t, J = 7.6 Hz, 1H), 7.66 (t, J = 6.9 Hz, 1H), 7.59 (d, J = 7.9 Hz, 1H), 6.90 (m, 2H), 4.23 (d, J = 16.5 Hz, 1H), 4.09 (d, J = 15.8 Hz, 2H), 3.88 (d, J = 15.8 Hz, 1H), 2.95 (br m, 4H), 2.36 (q, J = 7.5 Hz, 2H), 1.27 (s, 9H), 1.20 (t, J = 7.5 Hz, 3H); ^{13}C{^{1}H} NMR (CD_3CN, 75.6 MHz) δ 185.7, 156.6, 151.3, 148.9, 142.8, 142.5, 126.5, 126.1, 123.6, 116.8, 58.1, 57.5, 51.1, 42.0, 30.6, 29.2, 26.8, 13.6 (19 signals expected, 18 observed; two overlapping aromatic resonances at 156.6 ppm); FTIR (KBr, cm^{-1}) 1609, 1566, 1489, 1442, 1420, 1094 (ν_{ClO_4}), 623 (ν_{ClO_4}). Anal. Calcd for $C_{21}H_{29}N_4O_5SClZn$: C, 45.98; H, 5.33; N, 10.22. Found: C, 45.27; H, 5.56; N, 9.84.

Isolation and Characterization of *N*-((*N*,*N*-Diethylamino)-ethyl)-*N*-((6-amino-2-pyridyl)methyl)-*N*-((2-pyridyl)methyl)-amine (dappa). To a methanol (∼10 mL) solution of **4**$(OTf)_2$ (0.14 g, 0.19 mmol) was added a methanol solution (5 mL) of $Me_4NOH·5H_2O$ (0.033 g, 0.19 mmol), and the resulting cloudy mixture was refluxed under nitrogen for 48 h. After the solution was cooled to room temperature, excess NaCN (12 equiv) was added, and the resulting heterogeneous mixture was stirred for ∼2 h. After addition of ∼30 mL of H_2O, the solution was transferred to a separatory funnel, and ∼20 mL of CH_2Cl_2 was added. The organic fraction was then removed, and the aqueous phase was further extracted with two additional aliquots (∼20 mL) of CH_2Cl_2. The combined organic fractions were dried over Na_2SO_4 and filtered, and the solvent was removed under reduced pressure. A yellow-brown oil was obtained (50 mg, 85%): ^{1}H NMR (CD_3CN, 400 MHz) δ 8.48−8.46 (m, 1H), 7.72−7.66 (m, 1H), 7.53 (d, J = 7.8 Hz, 1H), 7.36 (t, J = 7.5 Hz, 1H), 7.20−7.17 (m, 1H), 6.75 (d, J = 7.3 Hz, 1H), 6.36 (d, J = 8.1 Hz, 1H), 4.87 (br, 2H, NH), 3.85 (s, 2H), 3.58 (s, 2H), 2.63 (br s, 4H), 2.51−2.48 (m, 4H), 0.94 (t, J = 7.2 Hz, 6H); ^{13}C{^{1}H} NMR (CD_3CN, 100 MHz) δ 161.3, 160.0, 159.2, 149.8, 138.8, 137.4, 123.9, 123.0, 112.9, 107.3, 61.5, 61.4, 52.8, 51.9, 48.1, 12.1 (16 signals expected and observed); LRFAB-MS (NBA) *m*/*z* (relative intensity) 314 ($[M + H]^+$, 3).

Recovery of Unaltered bdppa Ligand from Reaction of 6(OTf)$_2$ with Me$_4$NOH·5H$_2$O. To a methanol (∼4 mL) solution of **6**$(OTf)_2$ (0.29 g, 0.37 mmol) generated in situ was added a methanol solution (4 mL) of $Me_4NOH·5H_2O$ (0.069 g, 0.38 mmol), and the resulting cloudy solution was heated for 72 h at 40(1) °C. After the reaction mixture was cooled to room temperature, excess NaCN (0.22 g, 4.5 mmol) was added, and the resulting heterogeneous mixture was stirred for ∼2 h. During this time, all of the NaCN dissolved. After addition of water (10 mL) and 1 M NaOH (5 drops), the two-phase solution was extracted with CH_2Cl_2 (3 × 20 mL), and the combined organic fractions were dried over Na_2SO_4. Filtration of the solution, followed by removal of the solvent from the filtrate under reduced pressure, yielded a brown oil (0.15 g, 100%). This oil exhibited ^{1}H NMR features identical to those reported herein for the bdppa ligand.

Isolation and Characterization of *N*-((Ethylthio)ethyl)-*N*-((6-amino-2-pyridyl)methyl)-*N*-((2-pyridyl)methyl)amine (eappa). This compound was prepared and isolated in a manner analogous to that of dappa from an in situ generated methanol solution of [(epppa)Zn](OTf)$_2$ (**8**$(OTf)_2$) (yield 100%): ^{1}H NMR (CD_3CN, 400 MHz) δ 8.48−8.45 (m, 1H), 7.73−7.67 (m, 1H), 7.58 (d, J = 7.8 Hz, 1H), 7.38 (t, J = 7.8 Hz, 1H), 7.20−7.16 (m, 1H), 6.80 (d, J

= 7.3 Hz, 1H), 6.36 (d, J = 8.1 Hz, 1H), 4.77 (br, 2H), 3.79 (s, 2H), 3.58 (s, 2H); 2.75−2.60 (m, 4H), 2.43 (quartet, J = 7.4 Hz, 2H), 1.14 (t, J = 7.4 Hz, 3H); $^{13}C\{^1H\}$ NMR (CD_3CN, 100 MHz) δ 161.1, 160.0, 159.1, 149.8, 138.8, 137.3, 123.9, 123.0, 112.9, 107.3, 61.0, 60.9, 54.9. 29.7, 26.4, 15.4 (16 signals expected and observed); FTIR (KBr, cm^{-1}) 3328 (ν_{N-H}(asym)), 3174 (ν_{N-H}(symm)); EI-MS m/z (relative intensity) 302 ([M + H]$^+$, 100); HREI-MS m/z calcd for $C_{16}H_{22}N_4S$ 302.1565, found 302.1570.

Characterization of Initial Reaction Products Generated upon Treatment of 3(ClO$_4$)$_2$ with Me$_4$NOH·5H$_2$O in Acetonitrile. Characterization of [(bmppa$^-$)Zn]ClO$_4$ (10). A solution of **3**$(ClO_4)_2$ (0.062 g, 0.10 mmol) in dry acetonitrile (∼5 mL) was added to solid $Me_4NOH·5H_2O$ (0.018 g, 0.10 mmol). The resulting mixture was stirred for ∼30 min at room temperature under a nitrogen atmosphere. The solvent was then removed under vacuum. The remaining solid was dissolved in methylene chloride (∼7 mL). This solution was filtered through a Celite/glass wool plug, after which the filtrate was evaporated under reduced pressure to yield a pale yellow pasty material. This pasty solid was washed with Et_2O (3 × 4 mL), which left behind an off-white solid after drying. ^1H NMR analysis of this solid indicated the presence of free bmppa ligand and a new zinc complex (^1H NMR (CD_3CN, 400 MHz) δ 7.80 (br, 1H), 6.94 (br, 2H), 3.97 (br, 2H), 3.20−2.80 (br, 8H), 2.12 (s, 6H), 1.23 (s, 9H)). The ^1H NMR features of the zinc complex are suggestive of the formation of a deprotonated amide complex, [(bmppa$^-$)Zn]ClO$_4$ (**10**). Specifically, the upfield chemical shift position of two pyridyl protons (overlapped at 6.94 ppm) and the *tert*-butyl methyl resonance (1.23 ppm) are consistent with amide deprotonation.[4] The Et_2O wash portion contained only free bmppa ligand as indicated by ^1H NMR and thin layer chromatography.[6] In handling the proposed deprotonated amide complex in acetonitrile solution, we have found that it is unstable with respect to formation of the free ligand and presumably a zinc hydroxide/oxide inorganic species. Note: Formation of this deprotonated amide complex (as well as **5**, **7**, and **9**) requires the production of 1 equiv of Me_4NClO_4. We have previously isolated and quantified this salt in a reaction wherein **2** was generated via treatment of **1**$(ClO_4)_2$ with $Me_4NOH·5H_2O$ in methanol.[4]

X-ray Crystallography. A crystal of **4**$(ClO_4)_2$ was mounted on a glass fiber using a viscous oil. The sample was then transferred to a Nonius Kappa CCD diffractomer with Mo Kα radiation (λ = 0.71073 Å) for data collection at 150(1) K. Methods for determination of cell constants and unit cell refinement have been previously reported.[4] The structure was solved by a combination of direct methods and heavy atom methods using SIR97.[12] All nonhydrogen atoms were refined with anisotropic displacement coefficients. Complex **4**$(ClO_4)_2$ crystallizes in the triclinic crystal system in the space group $P\bar{1}$. All hydrogen atoms were located and refined independently.

A crystal of **8**$(ClO_4)_2$ was mounted in a similar fashion, and data were collected and refined as previously described.[4] All nonhydrogen atoms were refined with anisotropic displacement coefficients. Complex **8**$(ClO_4)_2$ crystallizes in the monoclinic crystal system in the space group $P2_1$. The Zn(II) ion was found to be disordered over two positions (Zn(1) and Zn(1A)). Refinement yielded an 85:15 ratio in occupancy for these two positions. The carbons of the −SEt substituent were also found to be disordered. Splitting of each into two fragments (C(20)/C(20A) and C(21)/C(21A)) and refinement yielded a 50:50 ratio in occupancy for each carbon center. All hydrogen atoms were assigned isotropic displacement coefficients U(H) = 1.2U(C) or 1.5U(C_{methyl}), and their coordinates were allowed to ride on their respective carbon using SHELXL97.[13]

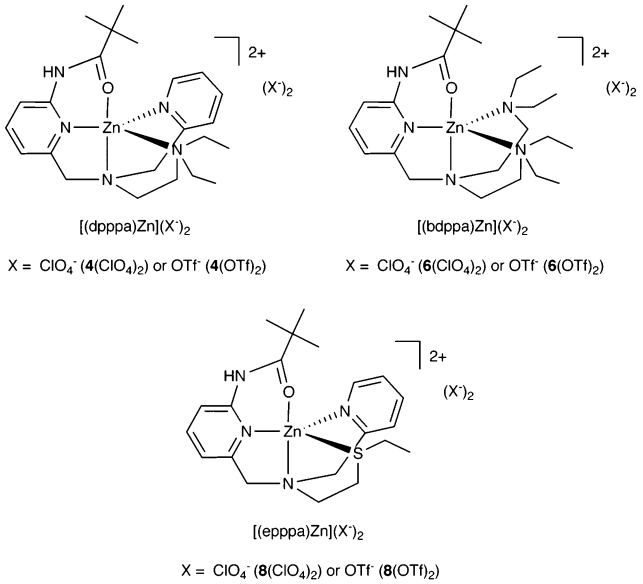

Figure 2. Drawings of the new amide-containing zinc complexes prepared in this study.

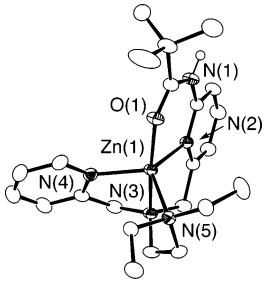

Figure 3. ORTEP drawing of the cationic portion of **4**$(ClO_4)_2$. All ellipsoids are drawn at the 50% level. Hydrogen atoms other than the amide proton are not shown for clarity.

Results

Synthesis and Characterization of Zinc(II) Complexes of New Amide-Appended Ligands. A series of zinc complexes of new amide-appended chelate ligands (Figure 2) have been prepared. An ORTEP drawing of the cationic portion of **4**$(ClO_4)_2$ is shown in Figure 3. Details of the X-ray data collection and refinement are given in Table 1. Selected bond distances and angles are given in Table 2. The zinc center in **4**$(ClO_4)_2$ has a distorted trigonal bipyramidal geometry (τ = 0.72), which is similar to that found for **1**$(ClO_4)_2$ (τ = 0.77).[4,14] The Zn(1)−O(1) bond length (2.0021(13) Å) in this complex is identical within experimental error to that found in **1**$(ClO_4)_2$[4] (2.008(3) Å; PF_6^- analogue,[2] Zn(1)−O(8), 2.0005(16) Å). The Zn(1)−N(5) bond distance (2.0881(16) Å) involving the *N*,*N*-diethylamino nitrogen donor is slightly longer than the Zn−N(py) distances in **1**$(ClO_4)_2$ (Zn(1)−N(4), 2.037(3) Å; Zn(1)−N(5),

(12) Altomare, A.; Burla, M. C.; Camalli, M.; Cascarano, G. L.; Giacovazzo, C.; Guagliardi, A.; Moliterni, A. G. G.; Polidori, G.; Spagna, R. *J. Appl. Crystallogr.* **1999**, *32*, 115−119.

(13) Sheldrick, G. M. *SHELXL-97. Program for the Refinement of Crystal Structures*; University of Göttingen: Göttingen, Germany, 1997.

(14) Addison, A. W.; Rao, T. N.; Reedijk, J.; van Rijn, J.; Verschoor, G. C. *J. Chem. Soc., Dalton Trans.* **1984**, 1349−1356.

Table 1. Summary of X-ray Data Collection and Refinement[a]

	4$(ClO_4)_2$	**8**$(ClO_4)_2$
empirical formula	$C_{23}H_{35}N_5Cl_2O_9Zn$	$C_{21}H_{30}N_4Cl_2O_9SZn$
fw	661.83	650.82
cryst syst	triclinic	Monoclinic
space group	$P\bar{1}$	$P2_1$
a (Å)	9.1080(2)	9.4708(9)
b (Å)	11.5504(2)	12.1353(8)
c (Å)	14.2834(4)	12.1290(11)
α (deg)	88.5940(14)	90
β (deg)	72.1198(10)	100.544(3)
γ (deg)	83.0280(13)	90
V (Å^3)	1419.35(6)	1370.5(2)
Z	2	2
density(calcd), Mg m^{-3}	1.549	1.577
temp (K)	150(1)	150(1)
cryst size (mm)	0.35 0.25 0.13	0.25 0.23 0.10
diffractometer	Nonius Kappa CCD	Nonius Kappa CCD
abs coeff (mm^{-1})	1.112	1.223
2θ max (deg)	54.96	54.90
completeness to 2θ (%)	99.2	99.3
no. of reflns collected	10166	5798
no. of independent reflns	6449	5798
no. of variable params	501	398
R1/wR2[b]	0.0326/0.0754	0.0767/0.1661
GOF (F^2)	1.033	1.040
largest diff (e Å^{-3})	0.380/−0.574	0.487/−0.429

[a] Radiation used: Mo Kα ($\lambda = 0.71073$ Å). [b] $R1 = \sum||F_o| - |F_c||/\sum|F_o|$; $wR2 = [\sum[w(F_o^2 - F_c^2)^2]/[\sum(F_o^2)^2]]^{1/2}$, where $w = 1/[\sigma^2(F_o^2) + (aP)^2 bP]$.

Table 2. Selected Bond Distances (Å) and Angles (deg) for **4**$(ClO_4)_2$[a]

Zn(1)−O(1)	2.0021(13)	O(1)−Zn(1)−N(4)	102.56(6)
Zn(1)−N(2)	2.0798(16)	O(1)−Zn(1)−N(2)	88.03(6)
Zn(1)−N(3)	2.1599(15)	N(4)−Zn(1)−N(2)	122.17(6)
Zn(1)−N(4)	2.0470(16)	O(1)−Zn(1)−N(5)	103.36(6)
Zn(1)−N(5)	2.0881(16)	N(4)−Zn(1)−N(5)	107.54(6)
		N(2)−Zn(1)−N(5)	125.13(6)
		O(1)−Zn(1)−N(3)	168.23(6)
		N(4)−Zn(1)−N(3)	80.75(6)
		N(2)−Zn(1)−N(3)	80.74(6)
		N(5)−Zn(1)−N(3)	86.13(6)

[a] Estimated standard deviations in the last significant figure are given in parentheses.

2.032(3) Å). Comparison of the bond angles involving the zinc centers in **4**$(ClO_4)_2$ and **1**$(ClO_4)_2$ revealed only minor differences, indicating that the presence of the $-NEt_2$ donor does not induce significant structural distortion within the equatorial plane of the cation.

One important structural feature of the cationic portion of **4**$(ClO_4)_2$ is reduced accessibility to the Zn(II) center relative to that found in **1**$(ClO_4)_2$. Examination of space-filling models of these cations indicates that the alkyl substituents of the NEt_2 donor in **4**$(ClO_4)_2$ provide steric hindrance in the N(4)−Zn(1)−N(5) and N(2)−Zn(1)−N(5) bond angles. Of relevance to amide cleavage chemistry, this means that **4**$(ClO_4)_2$ could potentially form a six-coordinate complex with a monodentate ligand (e.g., methoxide) only via approach in the N(2)−Zn(1)−N(4) angle, whereas in **1**$(ClO_4)_2$ this approach is feasible in various metal−ligand angles within the equatorial plane.

An ORTEP drawing of the cationic portion of **8**$(ClO_4)_2$ is shown in Figure 4. Details of the data collection and refinement are given in Table 1. Selected bond distances and angles are given in Table 3. Similar to **1**$(ClO_4)_2$ and **4**$(ClO_4)_2$, the zinc center in **8**$(ClO_4)_2$ has a distorted trigonal bipyramidal geometry ($\tau = 0.75$).[14] The Zn(1)−O(1) distance (1.998(7) Å) is identical within experimental error to that found in **1**$(ClO_4)_2$, **4**$(ClO_4)_2$, and [(beppa)Zn]$(ClO_4)_2$ (2.006(3) Å; beppa = *N*,*N*-bis(2-ethylthio)ethyl-*N*-((6-pivaloylamido-2-pyridylmethyl)amine), a complex supported by a N_2S_2 donor chelate ligand akin to that found in **3**$(ClO_4)_2$.[1] Similarly, the Zn(1)−N(2) distances (amide-appended pyridyl donor) and the Zn−N(3) distances (tertiary amine nitrogen) in this series of complexes (**1**$(ClO_4)_2$, **4**$(ClO_4)_2$, [(beppa)Zn]$(ClO_4)_2$, **8**$(ClO_4)_2$) differ by less than ∼0.06 Å. The Zn(1)−S(1) distance in **8**$(ClO_4)_2$ (2.399(3) Å) is approximately the average of the Zn−S bond distances in [(beppa)Zn]$(ClO_4)_2$ (2.366(1) and 2.427(1) Å).[1]

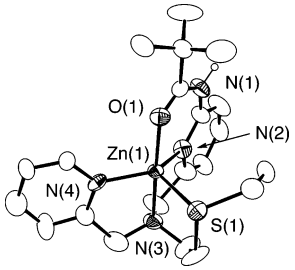

Figure 4. ORTEP drawing of the cationic portion of **8**$(ClO_4)_2$. All ellipsoids are drawn at the 30% level. Hydrogen atoms other than the amide proton are not shown for clarity.

Table 3. Selected Bond Distances (Å) and Angles (deg) for **8**$(ClO_4)_2$[a]

Zn(1)−O(1)	1.998(7)	O(1)−Zn(1)−N(4)	102.2(2)
Zn(1)−N(2)	2.021(7)	N(4)−Zn(1)−N(2)	125.6(3)
Zn(1)−N(3)	2.169(8)	O(1)−Zn(1)−N(2)	89.1(3)
Zn(1)−N(4)	1.983(8)	N(4)−Zn(1)−N(3)	81.2(3)
Zn(1)−S(1)	2.399(3)	O(1)−Zn(1)−N(3)	170.4(3)
		N(2)−Zn(1)−N(3)	81.7(3)
		N(4)−Zn(1)−S(1)	113.4(3)
		O(1)−Zn(1)−S(1)	98.3(2)
		N(2)−Zn(1)−S(1)	117.4(2)
		N(3)−Zn(1)−S(1)	88.5(2)

[a] Estimated standard deviations in the last significant figure are given in parentheses.

A summary of the equatorial bond angles of **1**$(ClO_4)_2$, **4**$(ClO_4)_2$, **8**$(ClO_4)_2$, and [(beppa)Zn]$(ClO_4)_2$ is shown in Figure 5.[1,4] The presence of the thioether sulfur donors in **8**$(ClO_4)_2$ produces a more open N(2)−Zn(1)−N(4) bond angle relative to that found in **1**$(ClO_4)_2$ and **4**$(ClO_4)_2$. The other equatorial bond angle involving the amide-appended pyridyl donor (N(2)) in **8**$(ClO_4)_2$ is more acute than the N(2)−Zn(1)−N(5) bond angles in **1**$(ClO_4)_2$ and **4**$(ClO_4)_2$. The thioether ethyl substituent of **8**$(ClO_4)_2$ is positioned in the region outlined by the N(2)−Zn(1)−S(1) bond angle (Figure 5, 117.4(2)°) and sterically shields the metal center on the N_2OS face of the trigonal bipyramidal Zn(II) center.

It is worth noting that the chemical shifts of the amide *tert*-butyl methyl and N*H* proton resonances and the amide C=O ^{13}C resonance are generally similar in **1**$(ClO_4)_2$, **4**$(ClO_4)_2$, **6**$(ClO_4)_2$, and **8**$(ClO_4)_2$ (Table S1, Supporting Information). The presence of two sulfur donors in [(beppa)Zn]$(ClO_4)_2$ and [(bmppa)Zn]$(ClO_4)_2$ (**3**$(ClO_4)_2$; bmppa = *N*,*N*-bis(2-methylthio)ethyl-*N*-((6-pivaloylamido-2-pyridylmethyl)amine) gives amide ^1H and ^{13}C resonances consistently upfield of those produced by N_4- or N_3S-supported complexes, albeit the affect is not dramatic.[1] Mareque Rivas

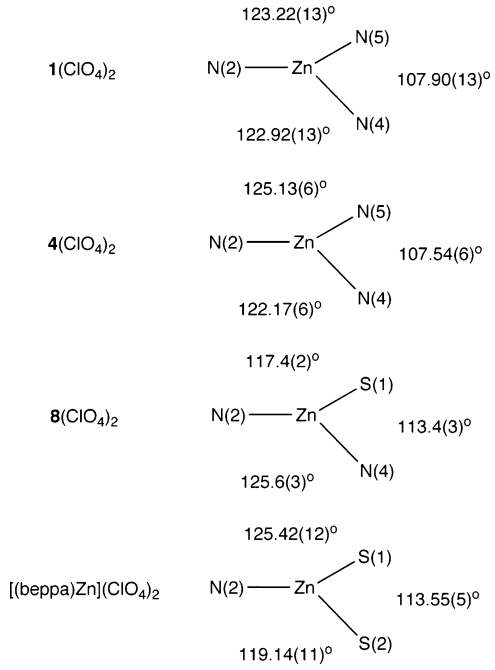

Figure 5. Comparison of equatorial bond angles in **1**$(ClO_4)_2$, **4**$(ClO_4)_2$, **8**$(ClO_4)_2$, and [(beppa)Zn]$(ClO_4)_2$.[1,4]

has argued that the difference in the chemical shift of the amide carbonyl carbon resonance in **1**$(ClO_4)_2$ versus [(bmppa)Zn]$(ClO_4)_2$ (~2 ppm) is an indication of the strength of $Zn-O_{amide}$ binding and hence amide activation by the Zn(II) center.[4] This argument has been used to rationalize why **1**$(ClO_4)_2$ exhibits a faster rate of amide methanolysis in basic methanol than does [(bmppa)Zn]$(ClO_4)_2$. We outline herein that, in addition to this proposed electronic effect, other factors likely also contribute to the differing rates of amide methanolysis of these complexes (vida infra).

Treatment of 4$(OTf)_2$, 6$(OTf)_2$, and 8$(OTf)_2$ with $Me_4NOH\cdot5H_2O$ in Methanol. Identification of Reaction Products. Admixture of equimolar amounts of **4**$(OTf)_2$ and $Me_4NOH\cdot5H_2O$ in methanol, followed by refluxing of the resulting solution under nitrogen for 48 h and workup using NaCN, yielded the primary amine-appended chelate dappa (*N*-((*N*,*N*-diethylamino)ethyl)-*N*-((6-amino-2-pyridyl)methyl)-*N*-((2-pyridyl)methyl)amine; Scheme 2) in 85% yield. Similarly, a reaction involving **8**$(OTf)_2$ and $Me_4NOH\cdot5H_2O$ yielded eappa (*N*-(ethylthio)ethyl-*N*-((6-amino-2-pyridyl)-methyl)-*N*-((2-pyridyl)methyl)amine) in quantitative yield. The proposed formation of Me_4NOTf and methyl trimethylacetate in these reactions is based on the similar reactivity of **1**$(ClO_4)_2$ wherein these types of byproducts have been isolated and/or quantified.[4] Interestingly, the same type of reaction involving **6**$(OTf)_2$ and $Me_4NOH\cdot5H_2O$, with heating at 313 K for 72 h and the standard NaCN workup, yielded only the unaltered bdppa ligand in quantitative yield. Thus, while amide methanolysis occurs for **4**$(OTf)_2$ and **8**$(OTf)_2$, no amide methanolysis takes place under similar conditions using [(bdppa)Zn]$(OTf)_2$ (**6**$(OTf)_2$). We note that we have previously reported that the N_2S_2O-ligated zinc complexes **3**$(ClO_4)_2$ and [(beppa)Zn]$(ClO_4)_2$ undergo reaction with $Me_4NOH\cdot5H_2O$ in methanol to yield amide methanolysis products (Scheme 3).[1]

Reactivity of 4$(ClO_4)_2$, 6$(ClO_4)_2$, 8$(ClO_4)_2$, and 3$(ClO_4)_2$ with $Me_4NOH\cdot5H_2O$. Characterization of the Deprotonated Amide Complexes [(dpppa$^-$)Zn]ClO_4 (5), [(bdppa$^-$)Zn]ClO_4 (7), and [(epppa$^-$)Zn]$(ClO_4)_2$ (9). Mechanistic studies of the amide methanolysis reaction of **1**$(ClO_4)_2$ revealed the involvement of a deprotonated amide intermediate (Scheme 1).[4] On the basis of the differing reaction products generated from the treatment of the N_4O-ligated zinc complexes **4**$(OTf)_2$, **6**$(OTf)_2$, and **8**$(OTf)_2$ with $Me_4NOH\cdot5H_2O$ in methanol−acetonitrile solution, we have investigated whether each complex forms a deprotonated amide complex. As shown in Scheme 4, treatment of **4**$(ClO_4)_2$ with an equimolar amount of $Me_4NOH\cdot5H_2O$ in methanol−acetonitrile (3:2) at ambient temperature followed by workup and precipitation of the zinc-containing product yielded [(dpppa$^-$)Zn]ClO_4 (**5**) in 64% yield. Similar deprotonated amide complexes [(bdppa$^-$)Zn]ClO_4 (**7**) and [(epppa$^-$)Zn]ClO_4 (**9**) (Scheme 4) were isolated from the reactions of **6**$(ClO_4)_2$ (generated in situ) and **8**$(ClO_4)_2$ with $Me_4NOH\cdot5H_2O$ in methanol−acetonitrile (3:2), respectively. Complexes **5**, **7**, and **9**, which are all off-white powders, were characterized by ^1H and ^{13}C NMR, FTIR, and elemental analysis.

The chemical shifts of the amide $-C(CH_3)_3$ and $C{=}O$ resonances of **2**, **5**, **7**, and **9** are given in Table S2, Supporting Information. In all cases these resonances are upfield of the corresponding resonances in the parent amide complexes (Table S1), which indicates an increase in the electron density present in the amide appendage.[4] Delocalization of the anionic charge into the adjacent pyridyl ring via resonance results in an upfield shift of two aromatic resonances, which for each deprotonated amide complex are found in the range of 7.0−6.8 ppm.[4] An NH resonance is not present in the ^1H NMR spectra of **5**, **7**, and **9** in dry CD_3CN.

Treatment of **3**$(ClO_4)_2$ with $Me_4NOH\cdot5H_2O$ in dry acetonitrile results in the formation of a mixture of two species. These are a free bmppa ligand and a new zinc complex. The ^1H NMR features of the zinc complex are suggestive of the formation of the deprotonated amide complex [(bmppa$^-$)Zn]ClO_4 (**10**). Specifically, the upfield shift of the *tert*-butyl methyl resonance (1.23 ppm) relative to its chemical shift position in the parent complex (1.38 ppm), and a new set of overlapping pyridyl proton resonances at 6.94 ppm, is consistent with amide deprotonation. In our initial paper on the chemistry of **3**$(ClO_4)_2$ and [(beppa)Zn]ClO_4 we reported the formation of two species, designated "**A**" and "**B**", immediately following the treatment of **3**$(ClO_4)_2$ with $Me_4NOH\cdot5H_2O$ in CD_3OD.[1] The chemical shifts of the *tert*-butyl resonances of **A** and **B** in CD_3OD were cited as 1.35 and 1.30 ppm, respectively.[1] Both signals are upfield of the chemical shift position of **3**$(ClO_4)_2$ in methanol (1.44 ppm). The **A** species (1.35 ppm) is tentatively assigned as the deprotonated amide complex on the basis of the upfield shift of the *tert*-butyl methyl resonance. The **B** species (1.30 ppm) has been conclusively identified as the free bmppa ligand via (1) comparison of the chemical shift of the *tert*-butyl resonance with an authentic sample of the ligand[6] and (2) thin layer chromatographic analysis (silica gel, 3:1 ethyl acetate−hexanes) of the **3**$(ClO_4)_2$/$Me_4NOH\cdot5H_2O$ reaction

Scheme 2

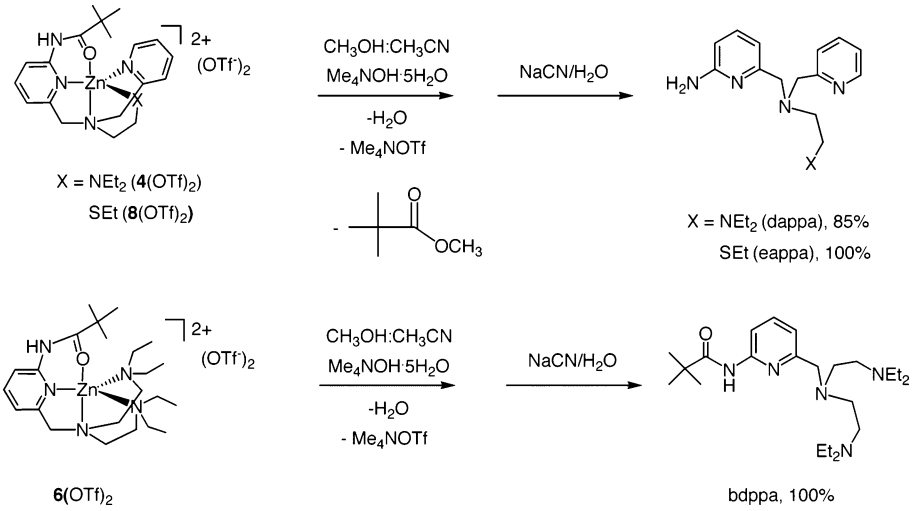

Scheme 3

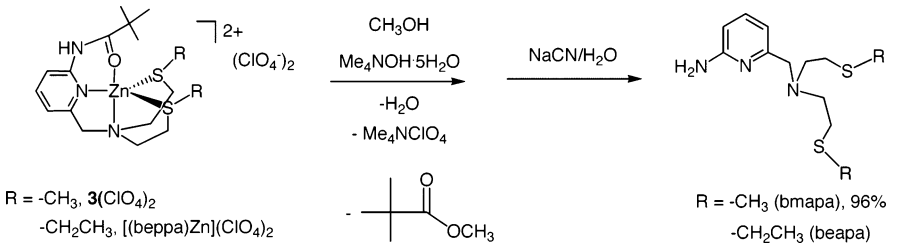

Scheme 4

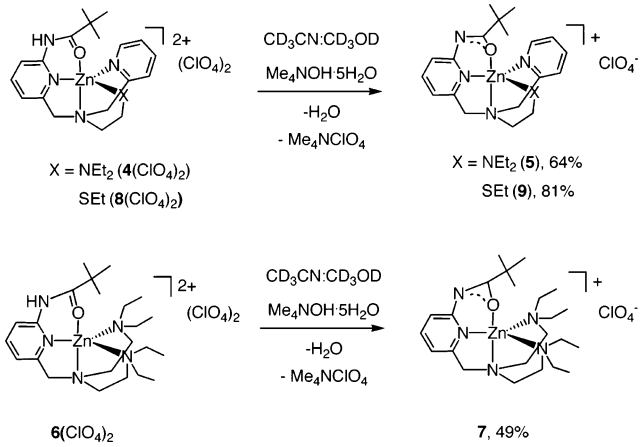

Scheme 5

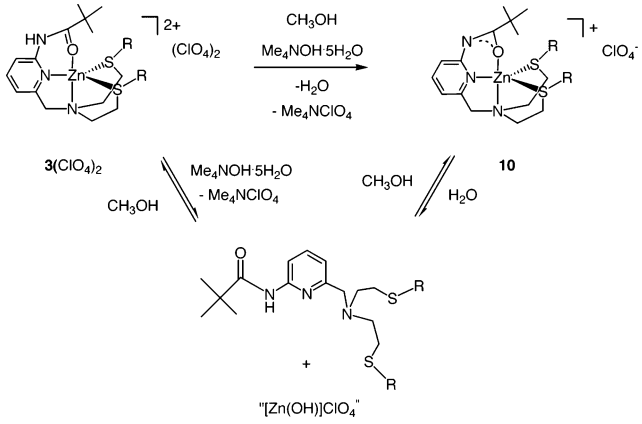

mixture in acetonitrile or methanol, which yielded a spot that moved in a fashion identical ($R_f \approx 0.88$) to that of the free ligand. We propose that the mixture of deprotonated amide complex (**A**) and free bmppa ligand (**B**) can be formed via one of two pathways (Scheme 5). Hydroxide ion could coordinate to the Zn(II) center of **3**$(ClO_4)_2$, resulting in ligand displacement. This may be feasible because of the weak donor properties of thioether ligands to Zn(II).[15] Alternatively, reaction of the deprotonated amide complex with water (from $Me_4NOH{\cdot}5H_2O$) could yield the same mixture involving free ligand and a zinc hydroxide salt ("[Zn(OH)]-ClO_4"). To date, we have been unable to characterize this proposed zinc hydroxide species, as it is present in a less than stoichiometric amount and another salt (Me_4NClO_4) of relatively low solubility is also formed in the reaction mixture. We have found that addition of excess base (4 equiv) to **3**$(ClO_4)_2$ in CD_3OD-CD_3CN leads to the quantitative release of the chelate ligand.

Kinetic Studies of the Amide Methanolysis Reactions of 4$(ClO_4)_2$ and 8$(ClO_4)_2$. In an approach identical to that employed for kinetic studies of **1**$(ClO_4)_2$,[4] we have collected rate data for the amide methanolysis reactions that occur upon treatment of **4**$(ClO_4)_2$ and **8**$(ClO_4)_2$ with $Me_4NOH{\cdot}5H_2O$ in CD_3CN-CD_3OD (3:5). For each reaction mixture, data were collected by ^1H NMR by monitoring the decrease in the intensity of the *tert*-butyl methyl resonance of the respective deprotonated amide intermediate complex [(dpppa$^-$)Zn]ClO_4 (**5**; $-C(CH_3)_3$, 1.30 ppm) or [(epppa$^-$)Zn]ClO_4 (**9**; $-C(CH_3)_3$, 1.27 ppm) as a function of time at a specific temperature.

(15) Grapperhaus, C. A.; Tuntulani, T.; Reibenspies, J. H.; Darensbourg, M. Y. *Inorg. Chem.* **1998**, *37*, 4052−4058.

Table 4. Rate Constants for Amide Methanolysis Reaction of $\mathbf{4}(ClO_4)_2$ in CD_3CN-CD_3OD

temp (K)	$[\mathbf{4}(ClO_4)_2]$ (M)	$[CD_3OD]$ (M)	k_{obsd} (s^{-1})	k_2 ($M^{-1}\,s^{-1}$)
318	0.020	15.39	$5.03(6) \times 10^{-6}$	$3.27(4) \times 10^{-7}$
328	0.020	15.39	$1.42(9) \times 10^{-5}$	$9.26(61) \times 10^{-7}$
338	0.020	15.39	$3.66(23) \times 10^{-5}$	$2.38(15) \times 10^{-6}$
348	0.020	15.39	$7.70(50) \times 10^{-5}$	$5.00(33) \times 10^{-6}$

Table 5. Rate Constants for Amide Methanolysis Reaction of $\mathbf{8}(ClO_4)_2$ in CD_3CN-CD_3OD

temp (K)	$[\mathbf{8}(ClO_4)_2]$ (M)	$[CD_3OD]$ (M)	k_{obsd} (s^{-1})	k_2 ($M^{-1}\,s^{-1}$)
298	0.020	15.39	$5.97(17) \times 10^{-5}$	$3.88(11) \times 10^{-6}$
308	0.020	15.39	$1.65(2) \times 10^{-4}$	$1.07(2) \times 10^{-5}$
318	0.020	15.39	$4.10(14) \times 10^{-4}$	$2.66(9) \times 10^{-5}$
328	0.020	15.39	$9.41(38) \times 10^{-4}$	$6.11(24) \times 10^{-5}$

Table 6. Thermodynamic Data for the Amide Methanolysis Reactions of $\mathbf{1}(ClO_4)_2$, $\mathbf{4}(ClO_4)_2$, and $\mathbf{8}(ClO_4)_2$

	$\mathbf{1}(ClO_4)_2$[a]	$\mathbf{4}(ClO_4)_2$[b]	$\mathbf{8}(ClO_4)_2$[b]
ΔH (kcal/mol)	15.0(3)	19.2(6)	17.3(2)
ΔS (cal/(mol·K))	−33(1)	−28(3)	−24(1)
$T\Delta S$[c] (kcal/mol)	−9.8(3)	−8.3(9)	−7.2(3)
ΔG[d] (kcal/mol)	24.8(6)	27.5(15)	24.5(5)

[a] Reference 4. [b] This work. [c] 298(1) K. [d] Calculated from $\Delta G^{\ddagger} = \Delta H^{\ddagger} - T\Delta S^{\ddagger}$ at 298(1) K.

Pseudo-first-order rate constants were determined from the slope of plots of ln $[\mathbf{5}]_t$ and ln $[\mathbf{9}]_t$ versus time. A typical correlation coefficient for these first-order plots was ≥0.996. The rate-determining step for the reaction involving $\mathbf{1}(ClO_4)_2$ has been previously shown to be second-order overall, with rate = $k[\mathbf{1}(ClO_4)_2][CD_3OD]$. Assuming a similar rate-determining step for the reactions involving $\mathbf{4}(ClO_4)_2$ and $\mathbf{8}(ClO_4)_2$, second-order rate constants were determined from pseudo-first-order constants using the known concentration of CD_3OD present (Tables 4 and 5).[11] Pseudo-first-order rate constants for amide methanolysis starting from the intermediate deprotonated amide species **5** ($6.96 \times 10^{-5}\ s^{-1}$ at 348 K) or **9** ($6.12 \times 10^{-5}\ s^{-1}$ at 298 K) are within experimental error of the average rate constants obtained starting from $\mathbf{4}(ClO_4)_2$ and $\mathbf{8}(ClO_4)_2$, thus indicating the deprotonated intermediate is produced prior to the rate-determining step of these amide methanolysis reactions.

Using data collected over a temperature range of 318−348 K ($\mathbf{4}(ClO_4)_2$) and 298−338 K ($\mathbf{8}(ClO_4)_2$), Eyring plots were constructed (Figure S1, Supporting Information). Thermodynamic parameters determined from these plots, and for the amide methanolysis reaction involving $\mathbf{1}(ClO_4)_2$, are given in Table 6.

Attempted Kinetic Studies of the Methanolysis Reaction of $\mathbf{3}(ClO_4)_2$. As described herein, the initial species produced in the reaction of $\mathbf{3}(ClO_4)_2$ with $Me_4NOH\cdot 5H_2O$ in methanol are the deprotonated amide complex $[(bmppa^-)Zn]ClO_4$ (**A**) and free bmppa (**B**) ligand. Over the course of the reaction, the integrated intensities of the *tert*-butyl methyl resonances for both the **A** and **B** species decline, whereas the signal for methyl trimethylacetate increases in intensity until it is the only *tert*-butyl methyl resonance present. Mareque Rivas has previously reported a half-life for this reaction (in methanol) at 348 K of 3.95 h.[3] We monitored the rate of disappearance of the deprotonated amide complex $[(bmppa^-)Zn]ClO_4$ (**10**) but found that the data yielded a nonlinear pseudo-first-order plot, indicating more complicated kinetic behavior than is found for $\mathbf{1}(ClO_4)_2$, $\mathbf{4}(ClO_4)_2$, and $\mathbf{8}(ClO_4)_2$.

Discussion

Amide cleavage reactions are catalyzed by a variety of metal-containing enzymes.[16,17] In many cases, these enzymes contain zinc as the active site metal ion. To date, very few studies have been reported of the mechanistic details of amide cleavage reactions promoted by well-characterized zinc complexes.[4,18,19] We have previously studied the system outlined in Scheme 1.[4] Notably, while this reaction pathway involves the formation of a deprotonated amide intermediate, which is not a biologically relevant species, the next proposed species in the reaction pathway, a zinc complex having both amide and $-OCD_3$ nucleophile coordination to the Zn(II) center, does have relevance to proposed reactive species in biological systems. Specifically, mechanistic pathways for amide hydrolysis have been proposed wherein both the substrate and nucleophile are coordinated to the same Zn(II) center.[20] To date, the chemical factors that influence the formation and reactivity of such zinc-bound amide/nucleophile structures have not been fully explored.

In the work described herein we have investigated how changes in the supporting chelate ligand affect the amide methanolysis reactivity of synthetic amide-appended zinc complexes. X-ray crystallographic studies of $\mathbf{4}(ClO_4)_2$ and $\mathbf{8}(ClO_4)_2$ revealed that a change in the nature of the donors in the chelate ligand affects the (1) accessibility of the zinc center to solvent and/or anions in the equatorial plane and (2) equatorial bond angles of the zinc center when thioether sulfur donors are present.

Amide methanolysis reactivity studies of $\mathbf{4}(ClO_4)_2$, $\mathbf{6}(ClO_4)_2$, and $\mathbf{8}(ClO_4)_2$ provided evidence that an equatorial coordination position must be accessible on the zinc center for amide cleavage reactivity.

Kinetic studies of the amide methanolysis reactions of $\mathbf{1}(ClO_4)_2$, $\mathbf{4}(ClO_4)_2$, and $\mathbf{8}(ClO_4)_2$ yielded second-order rate constants at 318 K that varied with the chelate ligand structure. The reaction involving $\mathbf{4}(ClO_4)_2$ ($3.27(4) \times 10^{-7}\ M^{-1}\,s^{-1}$) is considerably slower than the reaction involving $\mathbf{1}(ClO_4)_2$ ($1.54(8) \times 10^{-5}\ M^{-1}\,s^{-1}$), whereas the methanolysis reaction of $\mathbf{8}(ClO_4)_2$ ($2.66(9) \times 10^{-5}\ M^{-1}\,s^{-1}$) is ∼1.7 times faster than that of $\mathbf{1}(ClO_4)_2$. From the data shown in Table 6, it can be seen that the slower rate of amide methanolysis for $\mathbf{4}(ClO_4)_2$ is accompanied by an unfavorable 4.2 kcal/mol increase in the enthalpy of activation ($\Delta H^{\ddagger}$) which is offset by only a slightly more favorable (by 1.5 kcal/mol) $T\Delta S^{\ddagger}$ term. When both are considered in $\Delta G^{\ddagger}$, the free energy barrier is 2.7 kcal/mol higher for the reaction involving $\mathbf{4}(ClO_4)_2$ relative to that found for $\mathbf{1}(ClO_4)_2$. We propose that

(16) Parkin, G. *Chem. Rev.* **2004**, *104*, 699−767.
(17) Weston, J. *Chem. Rev.* **2005**, *105*, 2151−2174.
(18) Hegg, E. L.; Burstyn, J. N. *Coord. Chem. Rev.* **1988**, *173*, 133−165.
(19) Berreau, L. M. *Adv. Phys. Org. Chem.* **2006**, *41*, 79−181.
(20) Holz, R. C. *Coord. Chem. Rev.* **2002**, *232*, 5−26.

this increase in free energy of activation is due to enhanced steric crowding in the transition state due to the presence of the (diethylamino)alkyl substituents. In the reaction involving **8**$(ClO_4)_2$ a smaller increase in $\Delta H^{\ddagger}$ (2.3 kcal/mol) is paired with an entropically more favorable $T\Delta S^{\ddagger}$ term (by 2.6 kcal/mol), giving a $\Delta G^{\ddagger}$ value that is slightly more favorable than that found for the reaction of **1**$(ClO_4)_2$. This provides an explanation for why the amide methanolysis reaction of **8**$(ClO_4)_2$ is slightly faster than the reaction of **1**$(ClO_4)_2$. A small increase in $\Delta H^{\ddagger}$ is consistent with the presence of only one −SEt alkyl substituent in the equatorial plane, thus providing a zinc center of slightly greater steric hindrance than in **1**$(ClO_4)_2$ but less steric hindrance than is found in **4**$(ClO_4)_2$. We speculate that the more positive activation entropy may be associated with the presence of the thioether sulfur donor, which can undergo a change in the direction of −SR canting in solution via switching of the sulfur lone pair that interacts with the zinc center. Evidence for this type of fluxional thioether coordination was found in low-temperature ^{1}H NMR studies of the N_2S_2-supported complex [(bmppa)Zn]$(ClO_4)_2$ (**3**).[1] These combined kinetic and thermodynamic results provide evidence that the rate of amide methanolysis in these zinc complexes is affected by a change in the chelate ligand structure and more specifically the degree of steric hindrance in the equatorial plane of the zinc center. In the extremely sterically hindered case of **6**$(ClO_4)_2$, where all of the equatorial bond angles are sterically protected by diethylamino donor alkyl groups, we suggest that no amide methanolysis occurs because the required zinc methoxide species cannot form.

We also further examined the amide methanolysis reaction of [(bmppa)Zn]$(ClO_4)_2$ (**3**$(ClO_4)_2$).[1] We found that treatment of **3**$(ClO_4)_2$ with $Me_4NOH{\cdot}5H_2O$ results in the initial formation of a deprotonated amide species and free bmppa ligand. The fact that the reaction of **3**$(ClO_4)_2$ with $Me_4NOH{\cdot}5H_2O$ in methanol-containing solutions ultimately results in nearly quantitative amide methanolysis indicates that the reaction(s) involving chelate ligand displacement must be reversible, as the free ligand does not undergo amide methanolysis under these conditions.[1] We suggest that, like the other systems, the deprotonated amide complex can undergo reaction with methanol to yield a reactive zinc methoxide species and amide methanolysis products.

Though our results suggest that steric factors strongly influence the amide methanolysis reactivity of the complexes described herein, the electron-donating properties of the appendages in each chelate ligand may also be important. Studies of pK_a values of zinc-bound water molecules as a function of the supporting chelate ligand have demonstrated that, for neutral N_4 donor chelate ligands, the pK_a value for a $ZnOH_2$ moiety can vary up to 2.7 pK_a units.[21] While it is unclear whether this substantial range is due in part to counterion and/or solvent effects, changes in the nature of the donor atom would be expected to at least subtly affect the Lewis acidity of the zinc center. This modulation could affect the activation of the amide carbonyl (as has been suggested by Mareque Rivas) and/or the nucleophilicity of the bound methoxide anion in the complexes described herein.

Acknowledgment. This work was supported by the National Science Foundation (CAREER Award CHE-0094066).

Supporting Information Available: X-ray crystallographic (CIF) files for **4**$(ClO_4)_2$ and **8**$(ClO_4)_2$, spectroscopic characterization data for **4**$(OTf)_2$, **6**$(OTf)_2$, and **8**$(OTf)_2$, experimental details for product identification and kinetic studies of the amide methanolysis reactions, tables of NMR data for amide and deprotonated amide complexes, and Eyring plot for the amide methanolysis reactions of **4**$(ClO_4)_2$ and **8**$(ClO_4)_2$. This material is available free of charge via the Internet at http://pubs.acs.org.

IC062020T

(21) Berreau, L. M. In *Activation of Small Molecules*: *Organometallic and Bioinorganic Perspectives*; Tolman, W. B., Ed.; Wiley-VCH: Weinheim, Germany, 2006; see also references therein.